J. Synchrotron Rad. (1997). **4**, 279–286

A New High-Flux Chemical and Materials Crystallography Station at the SRS Daresbury. 1. Design, Construction and Test Results

Robert J. Cernik,[a,b]* William Clegg,[a,c] C. Richard A. Catlow,[d] Graham Bushnell-Wye,[a] John V. Flaherty,[a] G. Neville Greaves,[e] Ian Burrows,[a] David J. Taylor,[a] Simon J. Teat[a,c] and Mohammed Hamichi[a,d]

[a]CLRC Daresbury Laboratory, Warrington WA4 4AD, UK, [b]Department of Crystallography, Birkbeck College, Malet Street, London WC1E 7HX, UK, [c]Department of Chemistry, University of Newcastle, Newcastle upon Tyne NE1 7RU, UK, [d]The Royal Institution of Great Britain, 21 Albemarle Street, London W1X 4BS, UK, and [e]Department of Physics, University of Aberystwyth, Penglais, Aberystwyth, Ceredigion SY23 3BZ, UK. E-mail: r.j.cernik@dl.ac.uk

(*Received 13 February 1997; accepted 9 May 1997*)

A new single-crystal diffraction facility has been constructed on beamline 9 of the SRS at Daresbury Laboratory for the study of structural problems in chemistry and materials science. The station utilizes up to 3.8 mrad horizontally from the 5 T wiggler magnet which can be focused horizontally and vertically. The horizontal focusing is provided by a choice of gallium-cooled triangular bent Si (111) or Si (220) monochromators, giving a wavelength range from 0.3 to 1.5 Å. Focusing in the vertical plane is achieved by a cylindrically bent zerodur mirror with a 300 μm-thick palladium coating. The station is equipped with a modified Enraf–Nonius CAD-4 four-circle diffractometer and a Siemens SMART CCD area-detector system. High- and low-temperature facilities are available to cover the temperature range from about 80 to 1000 K. Early results on test compounds without optimization of the beam optics demonstrate that excellent refined structures can be obtained from samples giving diffraction patterns too weak to be measured with conventional laboratory X-ray sources, fulfilling a major objective of the project.

Keywords: instrumentation; microcrystal diffraction; chemical crystallography; weakly scattering materials; SRS station 9.8.

1. Introduction

We report the development of a new experimental station for single-crystal diffraction at Daresbury Laboratory with applications in chemical and materials sciences. The main purpose of the project is to provide a facility for the solution of difficult crystal structures. These problems are expected to come from a variety of sources. One of the largest sections of activity will come from the study of crystals with one or more dimensions on the micrometre scale, where the reflections are too weak to measure using standard single-crystal equipment with a conventional laboratory X-ray source. There will also be cases where larger crystals could be grown but a very small crystal is desirable to minimize absorption and extinction effects or for high-pressure studies. Examples will come from the whole range of chemistry and materials science and are likely to include microporous materials, polymer electrolytes, drug polymorphs, non-linear optical materials, ceramics and minerals. The new station will be able to study crystals that would formerly have been categorized as single powder grains. The possibilities of this approach have been demonstrated by Harding, Kariuki, Cernik & Cressey (1994) in the structure solution of the industrially important catalyst precursor material aurichalcite, and have been recently assessed in a review article by Harding (1996).

The tunability of synchrotron radiation can also be utilized to exploit anomalous dispersion effects, for example to distinguish elements of similar atomic number, and to collect single-crystal data at high energy for accurate electron density studies; recent studies have shown, for example, how careful data collection can reveal subtle structural effects at the onset of the superconducting phase transition in high T_c oxides (Molchonov *et al.*, 1994).

The station has been designed to collect data precisely and rapidly by using a CCD area detector or to collect data reflection by reflection using an adapted four-circle diffractometer with a scintillation counter. The latter approach will be adopted for high-pressure work using diamond-anvil cells or for monitoring individual reflections, for example during phase transitions. The intense reflections from the diamonds in pressure cells can cause severe damage to CCD detector systems. The modified diffractometer will provide full four-circle access to reciprocal

space and is the only facility capable of single-reflection counting at Daresbury. The CCD system is essentially the same as has been used routinely and successfully on a sealed-tube X-ray source at the University of Newcastle upon Tyne for over two years, delivering hundreds of high-quality data sets, and is now installed in many other laboratories worldwide. The new station bridges the gap between Daresbury Laboratory's protein crystallography facilities and the more materials-science-oriented crystallography stations.

The new station has been made possible by major UK Research Council (now EPSRC) funding to a consortium of academic users and Daresbury Laboratory (now CCLRC) staff to support its construction and commissioning. It is positioned on the original 5 T wiggler magnet of the SRS and is designated as station 9.8. It has been built on the site formerly occupied by the energy-dispersive diffraction station 9.7 (Clark, Cernik & Pattison, 1989). The new station will still be capable of carrying out white-beam powder diffraction and Laue crystallography formerly undertaken on station 9.7, but these functions are expected to occupy only about 20% of the time on the redeveloped station.

2. Beamline and station construction

The incident flux from the synchrotron can be attenuated either by a set of source slits situated 5.2 m from the tangent point or by a set of pre-monochromator slits situated at 10.3 m. The design of the two sets of slits is very similar, consisting of a series of apertures in a tungsten carbide plate mounted on a water-cooled copper block. A vertical drive unit comprises a motor-driven ball screw running in pre-loaded bearings. This is attached to a guide rail and carriage on which the slit assembly is mounted. The end of travel indication is provided by limit switches. The source and pre-monochromator slits are shown in Figs. 1(*a*) and 1(*b*), respectively. The offset design of the source slit enables it to be positioned in a very restricted space. There is a 6 mm diameter hole in both slit assemblies to allow the white beam to enter the hutch for the continued operation of energy-dispersive diffraction experiments.

The first optical element in the single-crystal diffraction facility, located just inside the experimental hutch, is the triangular bent gallium-cooled silicon monochromator. This is identical in design to the system installed on beamline 16.1 and has been described by Bliss *et al.* (1995). Briefly, the Si (111) bent triangular crystal is positioned 10.6 m from the tangent point and is capable of collecting a maximum of 3.8 mrad horizontally. The (111) crystal has an asymmetric cut of 1° allowing a small compression of the beam. The Si (111) crystal will cover the wavelength range 0.4–1.5 Å. If higher energies are required, an Si (220) monochromator with an asymmetric cut of 2° is available, and this will deliver wavelengths down to 0.3 Å. The calculated band-pass is of the order of 0.1%. Finite-element analysis of the curved crystal together with experience of operation on station 16.1 has shown that the crystal must be cooled. This is achieved with a Ga/In/Sn coolant (which is liquid at room temperature) heat exchanged by water-cooled copper pipes. Depending upon the radius of curvature a horizontal spot size of 2 mm can be achieved at any point on the energy spectrum. The power density varies as a function of energy but is never as severe as the 800 W case cited on station 16.1. A diagram of the monochromator is shown in Fig. 2; the triangular crystal is clamped at the wide end and bent into a cylindrical shape. The curvature of the monochromator is produced by a motor-driven cam at the pointed end. Just under 50% of the crystal is in contact with the Ga/In/Sn coolant and the heat extracted by the eutectic mixture is dissipated in the water-cooled Cu block. The whole mechanism has been designed for easy removal from the supporting Huber 410 rotary table. A turbo pump vacuum of 10^{-7} torr is maintained in the vessel. A set of vertical bellows allows sufficient flexibility on a vertical shaft to drive the crystal and its mount out of the way and allow the white beam into the hutch. The whole monochromator mount is easily demountable in order to minimize change-over time between monochromators.

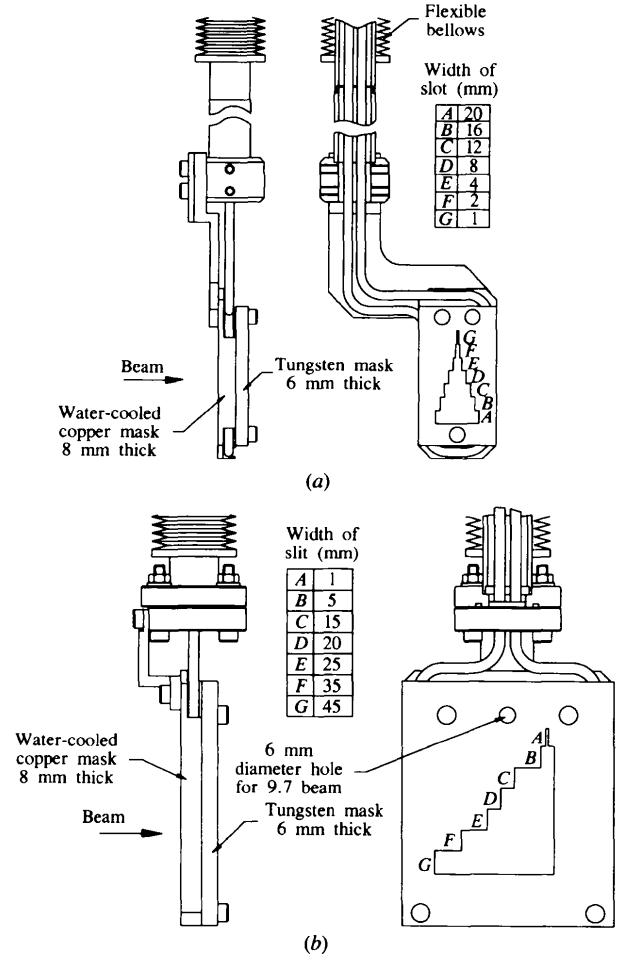

Figure 1
(*a*) The source slit assembly; (*b*) the pre-monochromator slit assembly.

The beam pipes in the hutch are of a modular nature. Each optical element is vacuum separated from its neighbour; this gives a robust, simple and flexible way of adapting to accommodate new experiments, or switching between existing experiments. The disadvantage is that there is a total of approximately 1.55 mm of Be window material in the beam path. Since the vast majority of the work is likely to be carried out at wavelengths around 0.7 Å (equivalent to Mo $K\alpha$ radiation) or less, this is not considered a significant problem, although applications at 1.5 Å will suffer from extra absorption of the incident beam.

The second optical element in the beamline is the mirror, shown in Fig. 3. The central bending mechanism provides an upward or downward thrust that is converted into a bending torque *via* the flexural pivots, push rods and four bar clamps at both ends of the mirror. All technical specifications for the mirror were exceeded by the manufacturers. The flat mirror has been manufactured from zerodur glass, coated with 300 μm of palladium and mounted in the assembly shown. The active width and length are 80 and 980 mm, respectively. The mirror has a sagittal slope error of less than 9 arcsec and a longitudinal

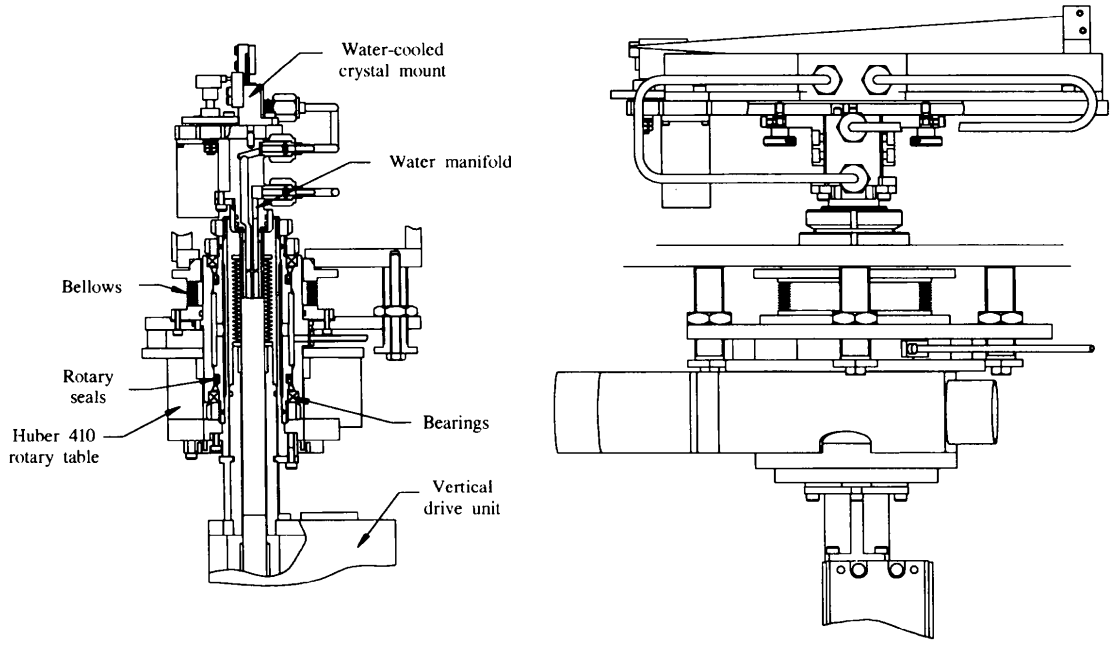

Figure 2
The triangular monochromator with its bending mechanism and mounting.

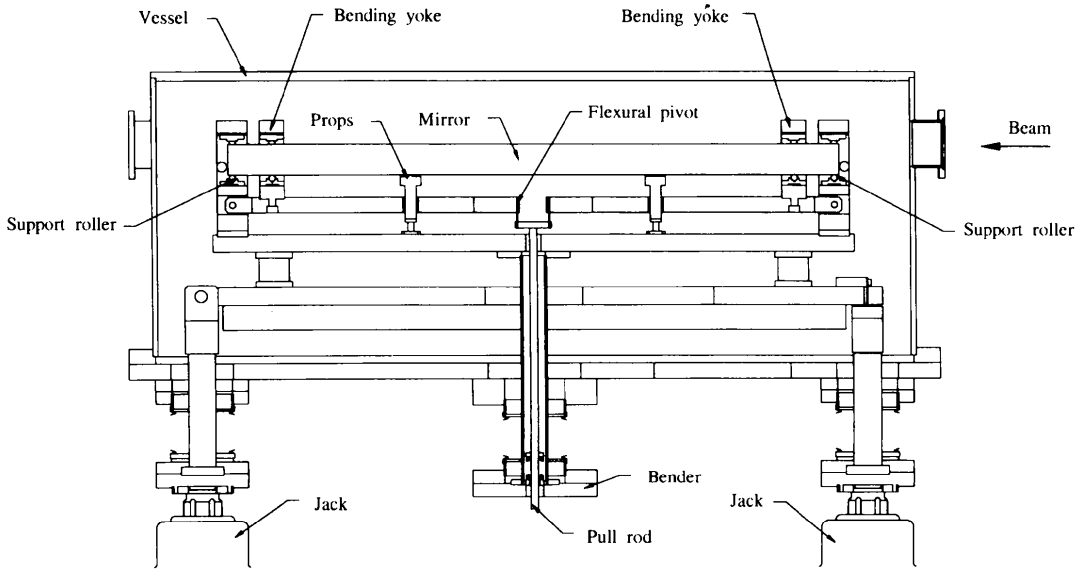

Figure 3
The mirror with its bending mechanism.

slope error of less than 1 arcsec. The mirror has been polished to a surface roughness that does not exceed 5 Å. The heat loading on the mirror is not severe since it only reflects the monochromatic beam, spread over much of its length. As well as vertical focusing, the mirror achieves rejection of wavelength harmonics, which are not reflected when the grazing angle is appropriately set. This is important for use with a CCD detector, which has no X-ray energy discrimination.

The two detector systems currently available are a Siemens SMART CCD area detector, complete with a three-circle fixed-χ goniometer and associated control electronics and software, and an Enraf–Nonius CAD-4 kappa-geometry diffractometer with a scintillation counter. Each of these is mounted perpendicular to the normal laboratory arrangement, so that the detector 2θ axis is horizontal instead of vertical, because of the polarization of the synchrotron beam. The SMART and CAD-4 systems have both been mounted on a table that provides vertical and lateral travel. The table can also pitch in order to accommodate the reflection upwards from the mirror, and allows rotational movement of the diffractometer whilst remaining rigid. There is one final set of manually adjustable slits before the diffractometer assembly and the sample mount. The SMART and CAD-4 both have their own proprietary collimator systems. The beam decay is monitored by a small ion chamber just after the final slit assembly, before the collimator. An Oxford Cryosystems Cryostream liquid-nitrogen cooler can be used in conjunction with either of the goniometer systems. Experiments at elevated temperatures are catered for by a modified Enraf–Nonius goniometer with a hot air jet attachment. The temperature of the heated filament is controlled by a simple thermistor current loop. For high-pressure work, miniature diamond anvils of the Merill–Basset type can be used as explained, for example, by Shulz & Sowa (1992). The distance from the tangent point to the monochromator pivot is 10670 mm, the distance from the pivot point to the mirror centre is 2365 mm and the distance from the mirror centre to the sample position on the SMART system is 3454 ± 50 mm in order to follow the beam focus.

The general assembly for the experimental hutch is shown in plan view in Fig. 4. The diffractometer and mirror pivot about the monochromator position on the large 2θ axis. This axis supports all the X-ray instrumentation in the hutch, including the powder and Laue experiments from station 9.7. The axis has a minimum angle into the shield wall of 7.26° and a swing range of 22.2°. These angles define the wavelength range available from the monochromator discussed earlier. The sideways deflecting geometry is necessary because of the restricted space on the beamline. The only drawback is that the 2θ axis must be moved every time the wavelength is changed. This necessitates realignments which are somewhat time-consuming but not difficult,

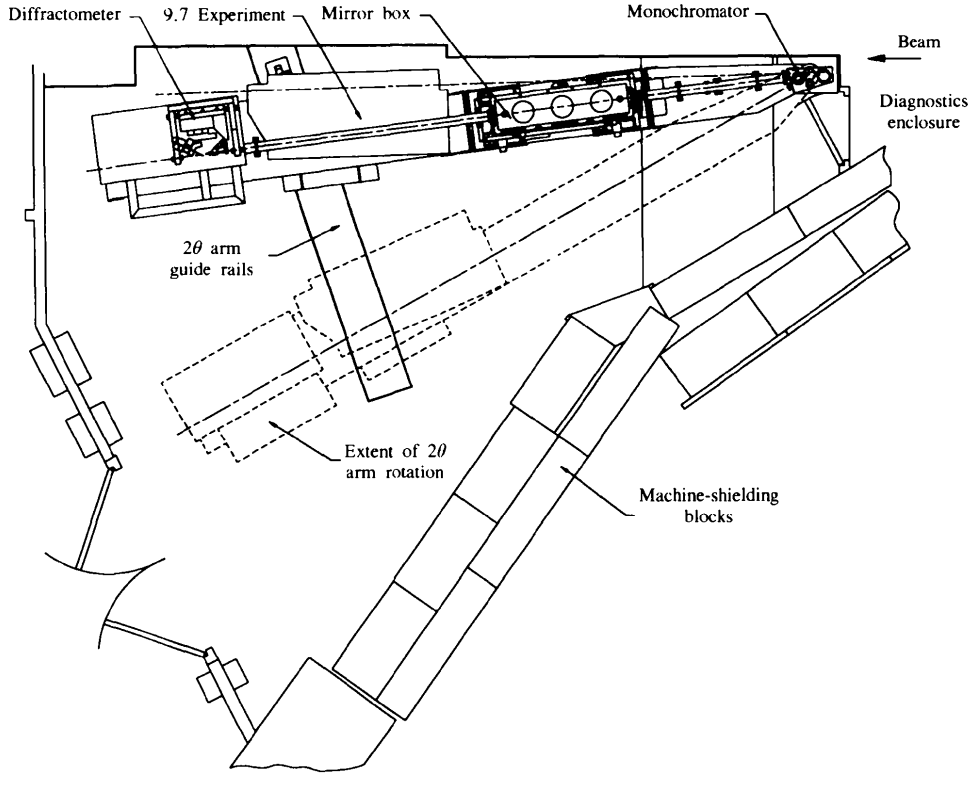

Figure 4
Plan of the experimental hutch for station 9.8, showing the large arm pivoting about the monochromator and carrying the mirror and diffractometer systems.

Table 1
Summary of the crystal and diffraction data for the four samples studied in the station trials.

Example	(1)	(2)	(3)	(4)
Chemical formula	$C_{67}H_{56}Cl_2O_5P_3Ru_2$	$C_{18}H_{17}NO_2$	$C_{72}H_{68}N_4O_{20}S_2$	$Mg_{0.18}Al_{0.82}PO_4$
Crystal size (mm)	0.14 × 0.14 × 0.14	0.25 × 0.16 × 0.03	0.30 × 0.12 × 0.10	0.04 × 0.04 × 0.04
Unit-cell volume (Å^3)	2809	1436	3256	4178
Scattering efficiency (e^2 Å^{-3})	6.3×10^{17}	7.0×10^{17}	5.1×10^{18}	9.9×10^{15}
Space group	$P\bar{1}$	$P2_1$	$P\bar{1}$	$P\bar{4}n2$
Z	2	4	2	10
Number of frames	1771	1771	2822	4813
Frame width (°)	0.3	0.3	0.2	0.1
Frame time (s)	5	3	5	5
Reflections measured	19080	9761	23612	26653
Unique reflections	9951	4831	11683	4094
Data with $F^2 > 2\sigma(F^2)$	7663	3939	8645	3494
Mean redundancy	1.9	2.0	2.0	6.5
R_{int}	0.039	0.026	0.036	0.049
Conventional R	0.051	0.046	0.093	0.067

and which preclude dynamic wavelength changes during an experiment, for example during MAD measurements. The operation currently takes about 4 h; however, this is being developed further to reduce the time.

Adjacent to the experimental hutch itself is a user area housing the control computers for the station optics, the alignment mechanisms and the diffractometer systems, as well as computing facilities for the analysis of the measured data. A high-power binocular microscope with rotating stage and polarizing analyzer is further enhanced by a pneumatic micromanipulator to aid the selection and mounting of very small crystals. Air-sensitive samples can be handled by standard inert-atmosphere Schlenk line techniques.

3. Diffractometer performance and test results

The new station became fully operational in October 1996, only a few weeks before a major scheduled shutdown for maintenance and development of the SRS. During this time it was possible to make an initial alignment of the optics and the SMART system and to collect data for about 30 samples chosen from a wide range of chemical and materials applications. All data were collected with a wavelength close to that of Mo $K\alpha$ (set approximately by reference to the Zr K-absorption edge and then calibrated as 0.6956 Å from the known cell parameters of a spherical ruby test crystal), for comparison with laboratory sources for some of the samples. Comparison of intensities indicates gains greater than 10^3 over rotating-anode sources, and these will be increased when the beam optics are further optimized. Some of the test data sets were from samples previously examined, successfully or otherwise, with laboratory sources. Conventional R factors as low as 0.018 have been obtained. Four particular examples, illustrative of the capabilities of the station, are given here; full details of the structures will be reported elsewhere. A summary of the relevant data is given in Table 1. The scattering efficiency is $\sum f^2 V_{crystal}/V_{cell}^2$ as defined by Harding (1996). The incident beam was restricted by a collimator to a 0.5 mm cross section, or less, as appropriate. Inspection of images of the strongly attenuated beam showed variations of around 0.5% in intensity across the sample dimension. Intensity normalization of exposed frames, to correct for synchrotron beam decay, absorption corrections and other effects, was carried out by the method of Blessing (1995). Analysis of initial frames repeated at the end of each data collection showed no significant effects caused by any changes in the incident beam other than the intensity decay. Polarization was assumed to be complete in the horizontal plane and was corrected for in the frame-integration and data-reduction procedures.

3.1. *Example (1): an organometallic complex*

This diruthenium complex (Fig. 5) had previously been examined on the Siemens SMART system at Newcastle upon Tyne, with a 3 kW Mo $K\alpha$ sealed-tube source. Crystals are very small and contain disordered solvent, giving weak diffraction. The original data collection took approximately 2 d and produced a result which was barely acceptable for publication, with a conventional R factor of 0.100 for 7378 reflections with $I > 2\sigma(I)$ (28920 reflections measured with $\theta_{max} = 25.0°$; 9857 unique data, $R_{int} = 0.108$) (Blenkiron *et al.*, 1997). The synchrotron data collection, at the same temperature of 160 K, used an even smaller crystal (approximately 5:1 volume ratio) and a total X-ray exposure time approximately 5% that of the original experiment. 19080 measured reflections with $\theta_{max} = 25.8°$ gave results much better from those of a conventional source. Standard uncertainties in the refined coordinates and anisotropic displacement parameters and in the derived geometrical parameters of interest (bond lengths and angles) are smaller than those of the original result by a factor of more than two. The molecular structure is shown in Fig. 6.

3.2. *Example (2): an organic compound*

This sample (Fig. 7) was submitted to the UK EPSRC-funded national crystallographic service at the University of Wales, Cardiff (Professor M. B. Hursthouse) for structure determination. Initial screening of crystals on an Enraf–Nonius FAST area-detector diffractometer with rotating-

anode Mo $K\alpha$ radiation showed no measurable diffraction data above about 10° in θ. The crystals are thin plates. Data were collected at 160 K on station 9.8 in under 6 h. The space group appeared to be either $P2_1$ or $P2_1/n$, depending on whether the relatively weak $h0l$ ($h + l$ odd) reflections were actually present or not, with four molecules per unit cell. The structure could be solved in $P2_1/n$, but twofold disorder of the epoxy ring had to be included in the refinement, and the value of R was about 0.08. In space group $P2_1$ there is no disorder and refinement proceeded smoothly to $R = 0.046$. The two independent molecules in the asymmetric unit (Fig. 8) are related by the pseudo glide plane. The quality of the synchrotron data is easily sufficient, not only to yield a structure from what would be immeasurably weak data by conventional methods, but even to resolve the pseudo-symmetry on the basis of a subset of the data with relatively low but significant intensity.

3.3. *Example (3): a supramolecular assembly*

This sample (Hamilton, Sanders, Davies, Clegg & Teat, 1997) also gave inadequate diffraction intensities when examined on a laboratory rotating-anode system (Rigaku *R*-AXIS-II image plate). It is composed of two molecular organic components (Fig. 9) which are synthesized in such a manner that they form a catenane; the self assembly of the pair of rings and the stacking of the molecules in the solid state are directed by graphitic π interactions of the aromatic segments. The structure contains severely disordered dimethyl sulfoxide solvent molecules, which are responsible to a large extent for the weak observed diffraction. A synchrotron data set was obtained overnight at 160 K. All non-H atoms of the two linked cyclic molecules were clearly revealed by a single direct-methods attempt. Refinement gave $R = 0.093$; the precision is undoubtedly limited by the difficulty of modelling the solvent disorder. The structure (without solvent) is shown in Fig. 10.

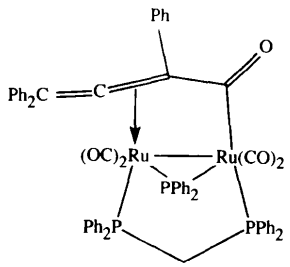

Figure 5
Example (1).

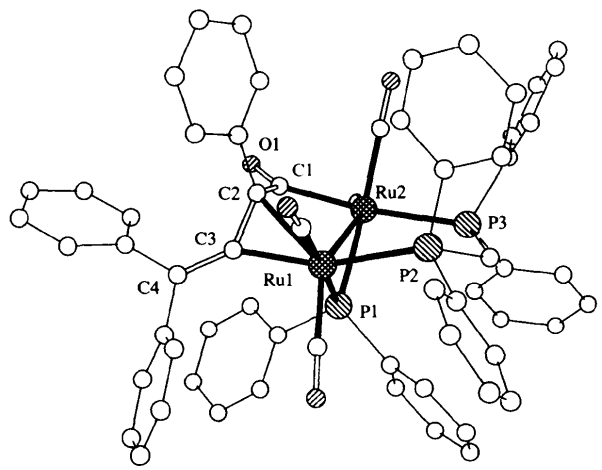

Figure 6
Molecular structure of the diruthenium complex [example (1)] without H atoms and disordered solvent.

3.4. *Example (4): a microporous magnesium aluminophosphate*

This microcrystalline sample, containing crystals of maximum dimension about 40 μm, is typical of many materials, such as zeolites, which are likely to form a substantial proportion of the samples to be studied on station 9.8. Designated STA-1, it has a large-pore framework of formula $Mg_{0.18}Al_{0.82}PO_4$. It forms in the presence of the template organic dication heptamethylene diquinuclidinium (Q), which is retained in the structure together with water, to give an overall formula $Mg_{0.18}Al_{0.82}PO_4.Q_{0.094}.0.22H_2O$ (Noble *et al.*, 1997). Overnight data were collected at 12 K as in the previous study. The framework atoms were refined anisotropically to $R = 0.067$, with separate and alternating sites for P and for disordered Mg/Al atoms. Residual electron density in the channels indicates the positions of template and water molecules, but these are highly disordered and unresolvable. Standard uncertainties in

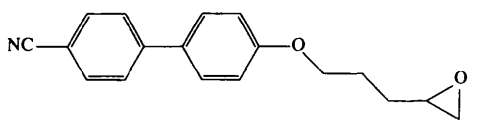

Figure 7
Example (2).

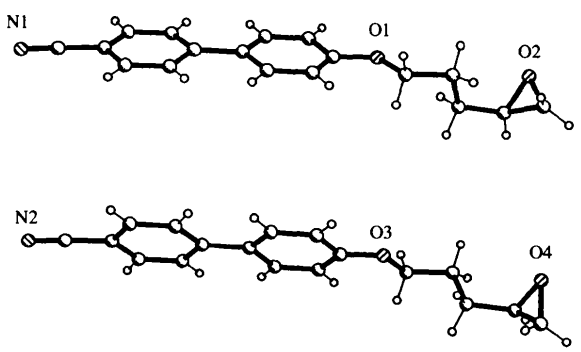

Figure 8
The two independent molecules of example (2) showing the pseudosymmetry broken by the different orientations of the epoxy groups.

framework bond lengths and angles are around 0.004 Å and 0.3°, respectively. The open framework structure is shown in Fig. 11. This result clearly demonstrates the capability of the station for the study of microcrystalline materials of this kind.

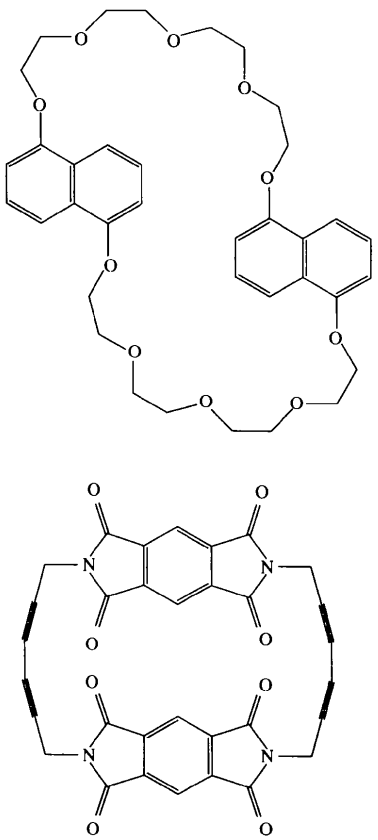

Figure 9
The separate molecular components of example (3).

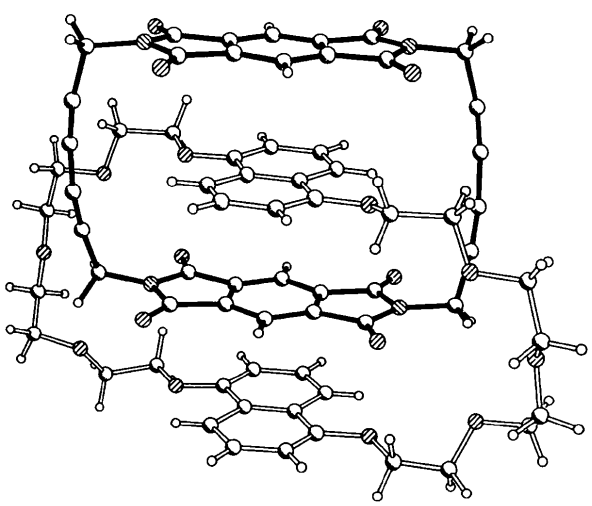

Figure 10
Structure of the catenane [example (3)] without the disordered solvent.

4. Conclusions

We have demonstrated with the examples shown above how the new station can significantly benefit the chemical and materials crystallography communities. In one case a direct comparison of laboratory and synchrotron data shows a significant improvement in the precision of the atomic parameters. Two of our examples show that by using synchrotron radiation structures can be determined from crystals that did not yield sufficiently good data from conventional sources to enable a crystal structure determination to be successful. Finally, a crystal structure has been determined from a crystal with a maximum dimension of 40 μm. Previous studies on crystals with 50 times lower scattering efficiency (Andrews *et al.*, 1988) than example (4) have been possible on the SRS wiggler source and an early generation of TV-type detector. Whilst the data from station 9.8 made it possible to solve the structure of example (4) compared with standard laboratory X-ray equipment, comparison of the scattering efficiencies of these samples indicates that the limit for structure determination from small crystals has not yet been reached, and that we can look forward to crystal studies of materials with yet smaller scattering power on station 9.8. Hence for the crystal structure example (4) a sample of about 10 μm in size would be tractable. Such a crystal size is typical for many microporous materials that in the past could only be studied by powder diffraction. The new station opens up the possibility of extending the range and complexity of the materials that can be studied into the fields of powder diffraction, high-pressure research, accurate electron density studies and perhaps the study of organically active peptides.

We thank EPSRC and CCLRC for the funding for this major project. The test crystals were kindly provided by Dr

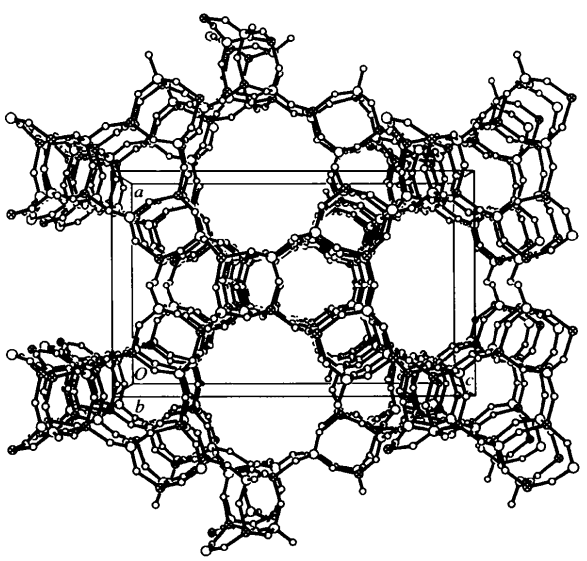

Figure 11
Structure of the framework of example (4), showing the large pores which contain disordered organic template and water molecules.

S. Doherty and Dr M. R. J. Elsegood (Newcastle) [sample (1)]; Dr I. A. Fallis, Professor M. B. Hursthouse and Dr S. J. Coles (Cardiff) [sample (2)]; Dr D. G. Hamilton, Professor J. K. M. Sanders and Dr J. E. Davies (Cambridge) [sample (3)]; Dr P. Lightfoot (St Andrews) [sample (4)].

References

Andrews, S. J., Papiz, M. Z., McMeeking, R., Blake, A. J., Lowe, B. M., Franklin, K. R., Helliwell, J. R. & Harding, M. M. (1988). *Acta Cryst.* B**44**, 73–77.

Blenkiron, P., Corrigan, J. F., Taylor, N. J., Carty, A. J., Doherty, S., Elsegood, M. R. J. & Clegg, W. (1997). *Organometallics*, A**16**, 297–300.

Blessing, R. H. (1995). *Acta Cryst.* A**51**, 33–38.

Bliss, N., Bordas, J., Fell, B. D., Harris, N. W., Helsby, W. I., Mant, G. R., Smith, W. & Towns-Andrews, E. (1995). *Rev. Sci. Instrum.* **66**, 1311–1313.

Clark, S. M., Cernik, R. J. & Pattison, P. (1989). *Rev. Sci. Instrum.* **60**, 2376–2379.

Hamilton, D. G., Sanders, J. K. M., Davies, J. E., Clegg, W. & Teat, S. J. (1997). *Chem. Commun.* pp. 897–898.

Harding, M. M. (1996). *J. Synchrotron Rad.* **3**, 250–259.

Harding, M. M., Kariuki, B., Cernik, R. J. & Cressey, G. (1994). *Acta Cryst.* B**50**, 673–676.

Molchonov, V., Tamazyou, R. A., Simonov, V. I., Blombery, M. K., Merisalo, M. J. & Mironov, V. (1994). *Physica C*, **229**, 3–4; 331–345.

Noble, G. W., Wright, P. A., Lightfoot, P., Morris, R. E., Hudson, K. J., Kvick, Å. & Graafsma, H. (1997). *Angew. Chem. Int. Ed. Engl.* **36**(1–2), 81–83.

Shulz, H. & Sowa, H. (1992). *High Pressure Res.* **8**, 661–666.